RSC Advances

ROYAL SOCIETY OF CHEMISTRY

www.rsc.org/advances

A new hybrid material resulting from the interaction of chitosan beads with a copper-naproxen metallodrug was prepared and characterized. The loaded beads were coated with Acrycoat, and investigated for release behavior in gastric/intestinal pH simulated solutions.

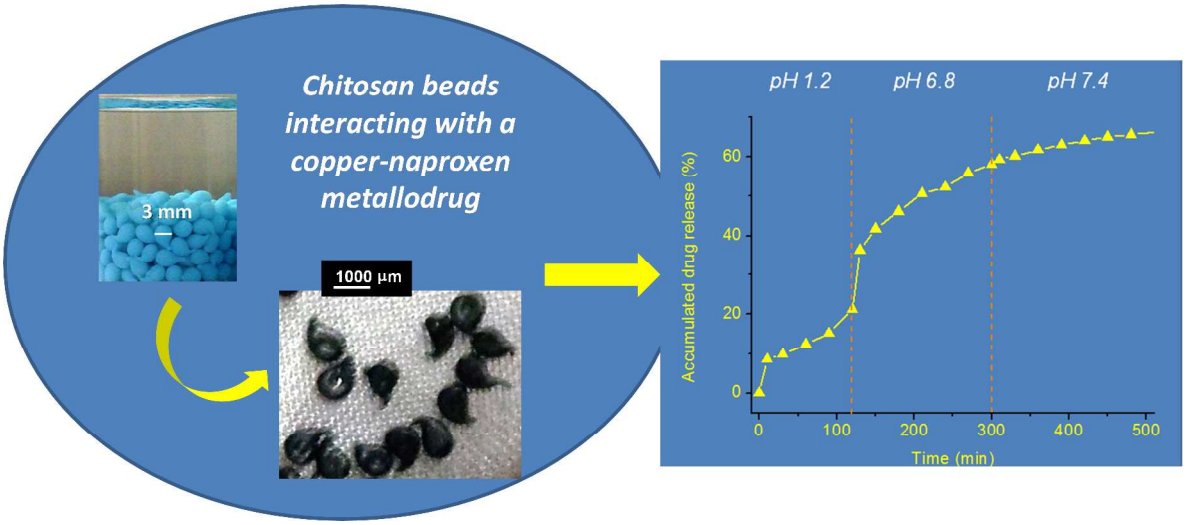

RSC Advances

ARTICLE

Interaction of chitosan beads with a copper-naproxen metallodrug

Received 00th January 20xx,
Accepted 00th January 20xx

DOI: 10.1039/x0xx00000x

www.rsc.org/

Douglas de J. Martins[§], Hanif-Ur-Rehman[§], Samara R. Alves Rico, Iguatinã de M. Costa, Andrea C. Pio Santos, Rachel G. Szszudlowski, Denise de Oliveira Silva[*]

This manuscript reports a novel hybrid system containing a copper-drug entrapped into the chitosan biopolymer. Chitosan beads (CTb) were prepared and investigated for interaction with a copper metallodrug (CuNpx) of the naproxen (HNpx) non-steroidal anti-inflammatory drug. The loading capacity of CTb for CuNpx suggests a sponge-like behavior for copper-drug entrapping at CuNpx concentration range from 10^{-4} to 10^{-2} mol L^{-1}. A novel CTb/CuNpx hybrid material formed by the copper-drug loaded into chitosan beads was prepared and characterized by elemental analysis, scanning electron microscopy, electronic absorption spectroscopy, FTIR spectroscopy, X-ray diffractometry and thermal analysis. The CTb/CuNpx hybrid material was coated with Acrycoat S100, and it was investigated for the behavior in gastric/intestinal pH simulated solutions to verify potential releasing properties. The coated beads showed capacity for releasing naproxen in a sustained release way for at least 24 h.

1. Introduction

Chitosan (CT) is a linear copolymer of (1,4-β-)-2-acetylamino-2-deoxy-d-glucopyranose and (1,4-β-)-2-amino-2-deoxy-d-glucopyranose (Fig. 1a), produced by partial deacetylation of the chitin extracted from crustaceans shells. [1,2] The biopolymer is well-known by its interesting physicochemical and biological characteristics, showing applications in a variety of fields, *e.g.*, pharmaceuticals, cosmetics, biomaterials, food, agriculturals and environment. [3-9] The unique biopharmaceutical properties, *i.e.*, biodegradability, biocompatibility, low toxicity and bioactivity, account for its relevant role in pharmaceutical and biomedical fields. [10-14] Chitosan, in different forms, *e.g.*, CT-beads, chemically modified-CT, and CT-based materials, has been studied for interactions with drugs, in particular for target delivery and drug controlled release. [15-20] CT-drug solid systems have been exploited to improve dissolution properties of poorly water-soluble drugs, *e.g.*, the naproxen non-steroidal anti-inflammatory drug (NSAID). [21] CT also shows ability of interacting with metal ions. The interaction of CT and CT-based materials with copper has been exploited for a variety of purposes, but having as the major focus the adsorption properties of the biopolymer for Cu(II) ions from common copper salt solutions. [22-30] Copper is an endogenous biometal and essential nutrient to the human body, and has been investigated for biological properties in the form of the corresponding metal complexes bearing a variety of ligands. The coordination of NSAID derived-carboxylates to metal ions has been used as strategy to develop new potential metallodrugs aiming the enhancement of efficacy of biological properties, *e.g.* anti-inflammatory and anticancer activity. [31-37] Cu-NSAIDs are capable of reducing gastrointestinal ulceration, in comparison to the severe side effects [38] caused by the corresponding NSAID parent drugs, while the anti-inflammatory activity is maintained upon NSAID coordination to the metal ion. [31-33] A number of Cu-NSAID complexes has been investigated in the past 30 years, [33] and the clinical relevance of these compounds is illustrated by the copper-indomethacin drug, which is used in veterinary clinic for the treatment of various inflammatory diseases in horses without showing toxic side effects after long term dosage. [39] Copper-naproxen complexes have also been suggested as potential antitumor agents. [34] Development of new formulations based on the interactions of Cu-NSAIDs with extended systems can be used as a strategy to improve pharmacological properties. [40] Taking into account the pharmacological potential of Cu-NSAIDs, and the fact that reports on chitosan interactions with metal coordination complexes are scarce, this work aims to contribute to the development on this field, by reporting studies on the interaction of the biopolymer with the metallodrug $[Cu_2(Npx)_4(dmso)_2]$ (Fig. 1b), where the $[Cu_2(Npx)_4]$

Departamento de Química Fundamental, Instituto de Química, Universidade de São Paulo. Av. Prof. Lineu Prestes, 748, B2T, 05508-000, São Paulo, SP, Brasil.
E-mail: deosilva@iq.usp.br. Tel: + 55-11- 30919124.

[§] *These authors have contributed equally to this work.*

dinuclear unit is named CuNpx, Npx = carboxylate derived from the naproxen NSAID (HNpx, Fig. 1c) and dmso = dimethylsulfoxide.

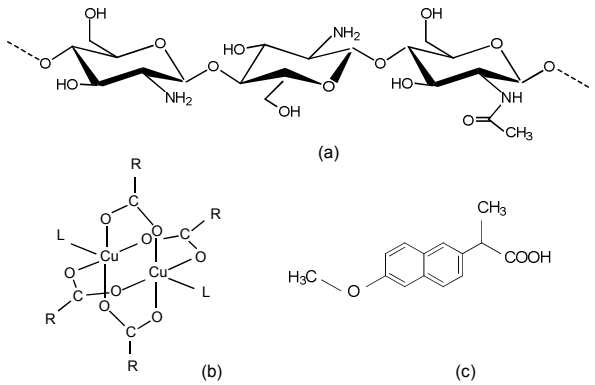

Fig. 1. Representation of the structures of: (a) chitosan - part of the CT polymeric chain where the unity on the right side expresses the acetylated groups remaining from chitin; (b) copper-naproxen metallodrug, where $RCOO^-$ = Npx , L = dmso, and the $[Cu_2(Npx)_4]$ dinuclear unit is named CuNpx; (c) naproxen (HNpx) non-steroidal anti-inflammatory drug.

2. Materials and Methods

2.1. Materials

Naproxen, HNpx (Natural Pharma, Brazil), copper acetate hydrate (Mallinckrodt), glutaraldehyde (GA) 25% (Sigma-Aldrich), liquid paraffin (Acros), Span 85 (Sigma), Acrycoat S100 (Corel Pharma Chem), and the organic solvents (Merck or Synth), were reagent grade and were used without further purification. Water was deionized. High molar mass chitosan was from Sigma-Aldrich, and the determined average viscosimetric molar mass and deacetylation medium degree (potentiometric titration) were 26 x 10^4 g mol^{-1} (26,000 Da) and 73%, respectively.

2.2. Preparation of $[Cu_2(Npx)_4(dmso)_2]$ or CuNpx-dmso

Copper acetate (2.00 g, 10.0 mmol Cu) dissolved in dmso (100 mL) was slowly added to a methanolic solution (75 mL) of HNpx (4.45 g, 20.0 mmol). The mixture was maintained at 60 °C under magnetic stirring for 1 h. After reaching the room temperature, dichloromethane (100 mL) was added to form a white precipitate which was removed by filtration. The solvent was allowed to evaporate, and green crystals were collected by filtration, washed with ethanol and dried in vacuum. Yield, 80 %. Anal. calc. (%) for $C_{60}H_{64}O_{14}S_2Cu_2$: C, 60.0; H, 5.4; Found: C, 59.5; H, 5.3. ESI-MS (m/z): 1067.2 ($\{[Cu_2(Npx)_4]+Na\}^+$ requires 1067.2). UV-VIS (nm): 700 (dmf/ethanol solution), ~ 674 (solid state). Major IR bands (cm^{-1}): (νCH) 3001, 2972, 2960, 2934; (ν_{as}COO) 1617; (νCC-ring) 1504; (ν_sCOO) 1409; (ν_{as}COC) 1270; (νSO) 1032. TG (°C)/mass loss (%): 30-200/13.0; 200-300/55.4; 300-600/17.3.

2.3. Preparation of CTb/CuNpx loaded-beads

CT (20.0 g) in 2 % acetic acid solution (700 mL) was slowly dropped into a NaOH solution (2.0 mol L^{-1}) through a peristaltic pump (5 mL h^{-1}). The formed beads were maintained under slow stirring in the basic solution for 24 h. After that, beads were washed with water until the washing water reached pH ~ 5. After being maintained in water for 24 h, beads were sieved and dried over a filter paper. In the sequence, 200 g of the beads were maintained under slow magnetic stirring in GA solution (100 mL, 0.1% GA in relation to commercial CT) for 4 days, and then they were washed with several portions of water. Amounts of 4.7 g of the these treated CT beads were individually added to CuNpx solutions of different concentrations at the range from 3.9 x 10^{-4} to 2.2 x 10^{-2} mol L^{-1}, in 1:9 v/v dmf : ethanol mixed-solvent (10 mL). These mixtures were maintained under periodical stirring at room temperature for 10 days. The formed blue beads were sieved, washed with ethanol, and dried in oven at 40 °C for 18 h, to give the dried greenish-blue CTb/CuNpx loaded-beads (0.20 - 0.40 g).

2.4. Preparation of CTb non-loaded-beads

The CTb non-loaded-beads were prepared by similar procedure to that described in item 2.3, but in the absence of CuNpx complex.

2.5. Preparation of coated CTb/CuNpx hybrid material

The CTb/CuNpx loaded-beads containing the maximum copper- and naproxen-loaded amounts, named as hybrid material, were coated with Acrycoat S100 using oil-in-oil solvent evaporation by a method adapted from the literature.[41] The beads were added to Acrycoat in acetone : ethanol (2 : 1 v/v), according to beads : Acrycoat : solvent ratio of 1.0 : 25 : 0.5 mg/mg/mL. The mixture was poured into light liquid paraffin (1 mg bead : 10 mL) containing Span 85 (1% w/v). The system was maintained at 150 rpm, for 3 h, at room temperature to allow solvent evaporation. The coated CTb/CuNpx loaded-beads were filtered, washed with n-hexane, and allowed to dry overnight in open atmosphere at room temperature. The mass increase in beads after coating was about 15%.

2.6. Behavior of the coated CTb/CuNpx hybrid material in gastric/intestinal pH simulated solutions

The investigation of the behavior of the coated CTb/CuNpx loaded-beads in gastric/intestinal pH simulated solutions was conducted on a PTWS 610 Dissolution Bath Apparatus from Pharma Test. The experiment was performed in duplicate using two individual batches of coated beads, which were independently coated with Acrycoat S100, and then introduced into sequential gastric/intestinal pH simulated solutions prepared according to the Pharmacopoeia. [42] In a typical experiment, the coated CTb/CuNpx loaded-beads (~ 90 mg), placed in the cylindrical basket attached to rotating spindle of the dissolution apparatus, were sequentially suspended in 200 mL of each of the following solutions: pH 1.2 hydrochloric acid solution for 2 h, pH 6.8 phosphate buffer for 3 h, and pH 7.4 phosphate buffer for 3 h. Between each of pH solution exchange, the beads were carefully rinsed with deionized water. The systems were maintained under 100 rpm, at 37.0 ± 0.5 °C. At pre-determined time intervals, volumes of 2.0 mL of the solutions were filtered through PVDF 0.22 μm Milex™ filters, and aliquots of 25 μL were used for HPLC assays. The medium was reconstituted

for volume by using the remaining volumes of samples. The sample at pH 7.4 was maintained for 24 h for HPLC final analysis.

2.7. Physical methods

The FTIR spectra of samples diluted in KBr were recorded on an ABB Bomen, MB-120, spectrophotometer having coupled diffuse reflectance accessory (Pike Technologies, Inc.). Electronic spectra of compounds in solution and solid state were recorded on Shimadzu UV-1650 PC and Guided-wave 260 (Analytical Spectral Devices, with optical fiber FieldSpec 3 Spectroradiometres) spectrophotometers, respectively. The X-ray diffractograms of powdered samples were registered on a Rigaku Diffractometer, Miniflex (Cu K_α, 1.5418 Å; 5 - 70°; 30 kV; step size 0.02°). High performance liquid chromatography (HPLC) was performed on a Shimadzu HPLC Prominence equipment having LC-20AT liquid chromatographer, SIL-20A auto sampler, SPD-M20A diode array detector and other Prominence modules. The reversed-phase HPLC procedure [42] was carried out with isocratic analysis, Lichrospher 100 RP-18 (5 µ, 250 x 4 mm) column, pH 4.0 buffered methanol/acetate (7:3, v/v) mobile phase, 25 µL injection volume, at 1 mL min^{-1} and 35 °C. Quantification of naproxen was based on a calibration curve previously determined by detection of the drug at 254 nm. Thermal analysis (TG-DSC-MS) studies were performed on a NETZSCH STA 409 PC Luxx thermobalance coupled to NETZSCH QMS 403C Aëolos (30-1000 °C; alumina crucibles; synthetic air atmosphere; 50 mL min^{-1}; 10 °C min^{-1}). Elemental analyses (Perkin-Elmer 2400 Elemental Analyzer), Cu analysis (Inductively Coupled Plasma Atomic Emission Spectroscopy (ICP-AES), Spectro - Arcos equipment, 324.754 nm), Electrospray Ionization Mass Spectrometry (ESI-MS) (Bruker Daltonics Micro TOF equipment, dry gas 4.0 L min^{-1}; 4 kV; 0.4 Bar; 180 °C) and Scanning Electron Microscopy (JEOL Neoscope JCM-5000 for SEM images of samples coated with gold) were performed at the Analytical Center of Institute of Chemistry, University of São Paulo.

3. Results and discussion

3.1. Preparation of the CuNpx metallodrug

The $[Cu_2(Npx)_4(dmso)_2]$ complex (named here as CuNpx-dmso) has been successfully prepared by an alternative method, in relation to that previously described, [43,44] by reacting copper-acetate directly with the HNpx drug without need of additional step for drug deprotonation. Complementary characterization of the solid compound and also of the complex dissolved in the mixed-solvent used in the interaction studies with CT is reported here for the first time. The spectroscopical characterization of the solid, discussed further, confirmed the structure as typical of dinuclear copper complex where the four Npx carboxylate equatorial ligands bridge two Cu(II) ions while the dmso ligands coordinated to the metal ions through oxygen atoms occupy the two axial positions. [43] The maintenance of the CuNpx dinuclear structure after dissolution of the complex in dmf : ethanol mixed-solvent was confirmed by the ESI mass spectrum in the positive mode (Fig. 2). The peak found at m/z 1067.2 (Fig. 2a) shows typical pattern of Cu isotopic distribution (Fig. 2b) which agrees with the simulated pattern (Fig. 2c) for the $\{[Cu_2(Npx)_4]+Na\}^+$ fragment (calc. m/z 1067.2; z = +1, where the Na^+ ion comes from the used experimental matrix).

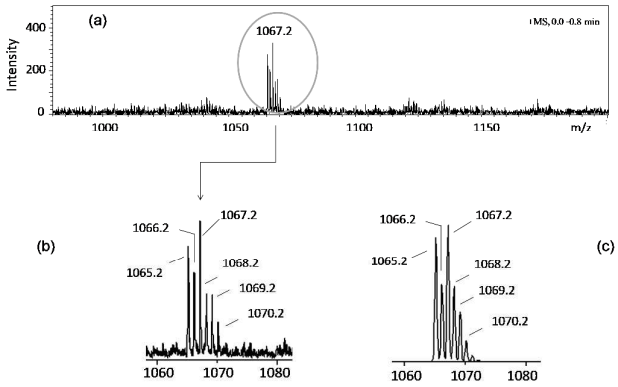

Fig. 2. (a) ESI mass spectrum registered for $[Cu_2(Npx)_4(dmso)_2]$ after dissolution in dmf/ethanol; (b) the ESI-MS isotopic pattern of the $\{[Cu_2(Npx)_4]+Na\}^+$ fragment (found m/z 1067.2); (c) ESI-MS simulated isotopic pattern of the $\{[Cu_2(Npx)_4]+Na\}^+$ fragment (calc. m/z 1067.2).

3.2. CTb loading capacity for CuNpx

The loading capacity of the CTb beads was analysed for both copper and naproxen. The amount of copper loaded into the beads (Fig. 3a) increases with increasing CuNpx concentration, to reach saturation at ~ 1.6 x 10^{-2} mol L^{-1}. The maximum loaded-copper amount was 8.5 x 10^{-4} mol Cu/g material (*i.e.*, 54 mg Cu per g of material). The plot of copper amount (mol of Cu) loaded into the CTb/CuNpx beads *versus* CuNpx concentration was linear (correlation coefficient, R^2 = 0.998) (Fig. 3b) and the loading efficiency, calculated by the expression {[(mol Cu_{loaded} – mol $Cu_{initial\ solution}$) / mol $Cu_{initial\ solution}$] x 100}, was 100 %. The plot of % loaded-naproxen (calculated on the basis of residual Npx determined by HPLC) as a function of CuNpx concentration (Fig. 3c) shows that CTb were able to load more than 70 % Npx (for the lowest CuNpx concentration) achieving saturation at ~ 92 %. The amount of loaded-Npx (mol) correlates well with the amount of loaded-Cu (mol) according to a linear tendency (Fig. 3d). Moreover, the CuNpx concentration (1.6 x 10^{-2} mol L^{-1}) at the saturation for loaded-metal is about twice its value (0.7 x 10^{-2} mol L^{-1}) at the saturation for the Npx drug, in agreement with the expected CuNpx : Cu : Npx molar ratio of 1:2:4.

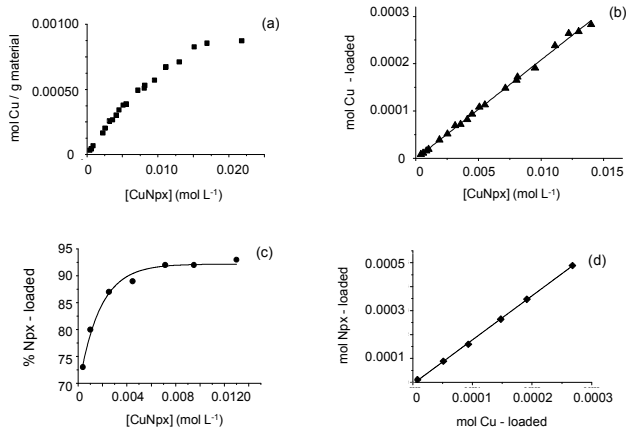

Fig. 3. (a) Copper-loading curve (mol of Cu / g material *vs.* CuNpx concentration); (b) total mol of Cu loaded into CTb *vs*. CuNpx concentration; (c) % Npx drug loaded into CTb *vs*. CuNpx concentration; (d) loaded-Npx *vs.* loaded-Cu (in mol).

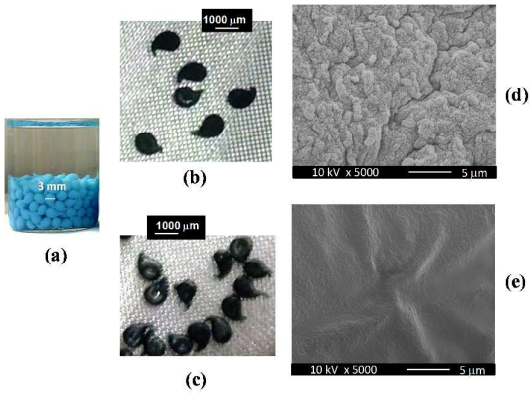

Fig. 4. Photographs of: (a) the CTb/CuNpx loaded-beads in the mother solution; (b) uncoated and (c) acrycoat-coated CTb/CuNpx beads of the hybrid material. SEM images of: (d) uncoated and (e) acrycoat-coated CTb/CuNpx beads of the hybrid material.

3.3. Composition/morphology of the CTb/CuNpx hybrid material

The CTb/CuNpx loaded-beads containing the maximum loaded-copper and loaded-naproxen amounts, named here as CTb/CuNpx hybrid material, were used for further studies. The material showed Anal. (%) Cu: 4.53; C: 47.1; H: 6.7; N: 6.0, and C/N ratio = 9 (based on the calculated amounts of C and N atoms per molar mass of CT (C: 39.9; N: 4.5 mol g^{-1}). An 8.0 % increase on the C content, in relation to CT as supplied (Anal. (%) C: 39.1; H: 6.7; N: 7.0, C/N ratio = 7; C: 32.5; N: 4.7 N mol g^{-1}) could be mostly associated to the naproxen loading. The low content of S (found < 0.3%) suggests that the dmso ligands were predominantly lost by dissociation during the interaction of the copper-drug with CTb. The composition (w/w) of the CTb/CuNpx hybrid material was estimated as 4.5 % Cu (ICP data); 30 % Npx; and 65.5 % CT matrix. In the original mother solution, the blue CTb/CuNpx loaded-beads of about 3 mm medium diameter showed an approximately spherical shape that is better described as a pear-like shape, with apparent homogeneous smooth surface (Fig. 4a). After dried in oven, the beads exhibited greenish-blue colour, and retained the pear-like shape, but the size was reduced to about 1000 µm medium diameter (Fig. 4b). The slightly rough surface with a collapsed center having small wrinkles might be associated to a partial collapse of the polymer network during dehydration.[45] The shape and the color of the beads were mostly preserved after they were coated with Acrycoat S100 (Fig. 4c). The effect of the acrycoat-coating process on the surface morphology is revealed by the SEM micrographs that show a porous morphology for the uncoated beads (Fig. 4d) in contrast to a more homogeneous surface morphology for the corresponding coated beads (Fig. 4e)

3.4. Electronic absorption spectra

The electronic absorption spectra of the CTb/CuNpx hybrid material, CuNpx-dmso in the solid state, and CuNpx-dmso in dmf/ethanol solution are shown in Fig. 5. The CuNpx-dmso complex in dmf/ethanol solution (Fig. 5a) shows one visible band at λ_{max} 700 nm, which can be assigned to the Cu(II) *d-d* electronic transition (band I, $d_{xz,yz} \rightarrow d_{x^2-y^2}$). The appearing of a shoulder at ~ 360 nm observed at the UV region could be associated to band II (charge transfer from the carboxylate-oxygen atoms to the metal ion) [46], in agreement with the carboxylate-bridged structure, thus giving evidence for the presence of the dinuclear species in the mixed-solvent. The CuNpx-dmso complex in the solid state shows a broader visible band ($d_{xz,yz} \rightarrow d_{x^2-y^2}$) shifted to λ_{max} ~ 674 nm, that is accompanied by a shoulder at lower energy ($d_{z^2} \rightarrow d_{x^2-y^2}$). The spectrum in solution may be assigned to the dinuclear species with the axially-coordinated dmso ligands, while the broadness and the higher energy shift of the visible band for the solid complex approaches the behaviour found for polymeric species, [47] probably due to the stronger character of the Cu-$O_{carboxylate}$ bonds compared to the Cu-O_{dmso} axial bonds. [46] In the spectrum of the CTb/CuNpx hybrid material, the visible band is even broader compared to the spectrum of the solid CuNpx-dmso. However, the λ_{max} is centered at ~ 700 nm. The spectra of the solids were tentatively de-convoluted to give three bands, in agreement with the findings for other Cu analogous compounds. [48,49] The values of λ_{max} for the de-convoluted bands were 623, 762, 986 nm for CuNpx-dmso, and 610, 762, 982 nm for the CTb/CuNpx hybrid material. The de-convolution suggests an energy shift of the visible band for the CTb/CuNpx hybrid material compared to the CuNpx-dmso complex that might be related to the interaction of copper with the amino groups of chitosan.

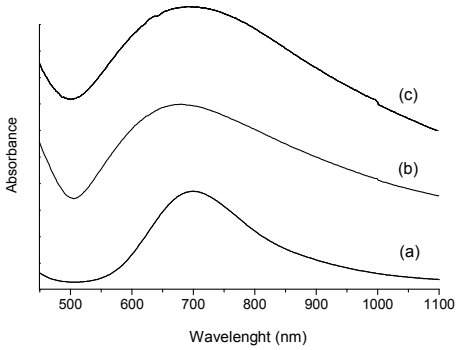

Fig. 5. Electronic absorption spectra at the visible region for: (a) CuNpx-dmso complex in dmf:ethanol (1:9 v/v) mixed-solvent; (b) CuNpx-dmso complex in the solid state;. (c) CTb/CuNpx hybrid material.

3.5. Infrared spectra

The FTIR spectra, at the region 4000 – 400 cm^{-1} (Fig. 6), of CTb non-loaded-beads, CTb/CuNpx hybrid material, CuNpx-dmso and HNpx were investigated. The non-loaded CTb (Fig. 6a), exhibits a broad intense band at ~ 3460 cm^{-1} that is ascribed to N-H stretching superimposed to O-H stretching vibrations involved in hydrogen bonds of the polysaccharide. [1] The bands appearing at 2923 and 2878 cm^{-1} were assigned to C-H stretching vibrations; the intensity ratio was slightly lower than that found for the dried commercial CT, indicating the presence of GA.[50] Bands of acetamide group which remained in the CT structure after the partial deacetylation of chitin were found at the region 1660-1610 cm^{-1}. The band at 1653 cm^{-1} could be assigned to the C=O stretching vibration of secondary amide group (amide I band). The shoulders at 1620-1590 cm^{-1} were ascribed to N-H bending vibrations of the NH_2 group, and that at ~ 1560 cm^{-1} to N-H deformation vibrations (amide II band). [1] The shoulder at ~ 1630 cm^{-1} may be due to the C=N stretching of imine group of crosslinking bonds with GA.[50] The FTIR spectrum of the CTb/CuNpx hybrid material shows significant changes (Fig. 6b), compared to the spectrum of the non-loaded CTb. The band at 3000-3700 cm^{-1} is broader for CTb/CuNpx, probably due to a disrupting of hydrogen bonds by the presence of the metal complex. [6] The band assigned to O-H and N-H vibrations shifts to 3450 cm^{-1}, and it is accompanied by a shoulder at 3250 cm^{-1}, suggesting coordination of the amino groups to the copper ions, since this region is typical of amine stretching vibrations. [6] A band at 2967 cm^{-1} was assigned to C-H stretching of naproxen, while the bands at 2930 and 2885 cm^{-1} were related to overlap of both CT and naproxen C-H stretching vibrations. The CTb/CuNpx hybrid material also shows typical bands of the CT at the region 2000-400 cm^{-1}. The major significant change, compared to the spectrum of the non-loaded CTb, is the higher intensity of the band assigned to the N-H deformation at 1565 cm^{-1}, which suggests interaction of the amino group with copper. [51] In addition, the spectrum of CTb/CuNpx shows the characteristic vibrational bands of the CuNpx unity. The bands at 1605 and 1416 cm^{-1}, which are absent in the non-loaded CTb spectrum, may be assigned to the Npx ligand, *i.e.*, COO asymmetric (ν_{as}COO) and symmetric (ν_{s}COO) stretching vibrations, respectively. The shift to lower (ν_{as}COO) and higher (ν_{s}COO) frequencies, compared to those found for the CuNpx-dmso complex (1617 and 1409 cm^{-1}, respectively, Fig. 6c), thus suggests an effect of axial ligand substitution. The values of $\Delta\nu$ (= ν_{as}COO - ν_{s}COO) are 189 and 208 cm^{-1} for CTb/CuNpx and CuNpx-dmso, respectively, both in the range observed for copper-carboxylates, thus confirming the dinuclear structure. [52] Moreover, these two bands are absent in the spectrum of HNpx (Fig. 6d) which, instead, shows typical bands of carboxylic acid, *i.e.*, C=O carbonyl stretching at 1728 cm^{-1} and C-O-H deformation at 1685 cm^{-1}. The detection of the S=O stretching vibration of the dmso ligand, which appears at 1032 cm^{-1} for CuNpx-dmso (Fig. 6c), might eventually be hampered for the CTb/CuNpx hybrid material due to overlap with CT bands. However, since no significant change in both frequency and shape of CT bands was observed at this region, and also the % S found for the hybrid material was negligible it is plausible to assume that the dmso ligands were replaced by the amino groups of CTb when the copper-drug interacted with the CTb.

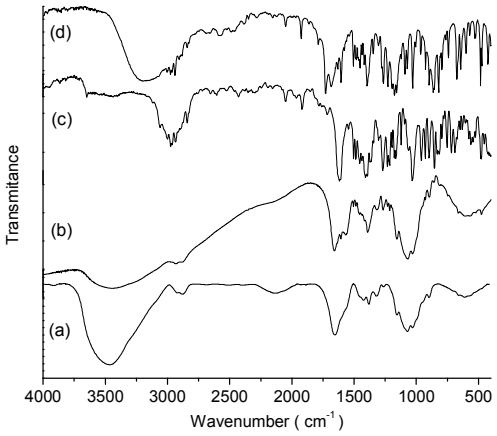

Fig. 6. FTIR spectra of: (a) CTb; (b) CTb/CuNpx hybrid material; (c) CuNpx-dmso; (d) HNpx.

3.6. X-ray diffraction

The XRD patterns of CTb/CuNpx hybrid material, CT (commercial), CTb non-loaded beads, CuNpx-dmso and HNpx are shown in Fig. 7. CT (Fig. 7a) exhibits two main peaks at 2θ values 20.3° (*d*-spacing = 4.4 Å) and 11.8° (*d* = 7.5 Å), which may be related to the regular crystal lattice (100 reflection) and hydrated crystals (020 reflection), respectively.[53-56] The incorporation of water molecules is favored by a highly ordered network formed by hydrogen bonds between acetamide-residues of neighboring chains. [55] The non-loaded CTb (Fig. 7b) shows no significant changes on both the relative crystallinity and the 100 reflection, compared to CT. The peak associated to the hydrated crystals, however, shifts to ~ 10.3° (larger *d*, ~ 8.6 Å) probably due to the presence of the GA. The CTb/CuNpx XRD pattern (Fig. 7c) reveals significant changes compared to the others. The decrease on the crystallinity may be

related to an effect on inter- and intra-chain hydrogen bonds of CTb after the copper-drug loading. The 020 reflection shifts to lower 2θ (~ 10.9°; *d* ~ 8.1 Å) probably due to small structural changes. Interestingly, the new material also shows an additional peak at lower 2θ value (6.5°) that corresponds to a larger *d*-spacing (13.3 Å). To try to elucidate this reflection, the CTb/CuNpx pattern was firstly compared to that of CuNpx-dmso. The absence of the highest intensity peaks of CuNpx-dmso (Fig. 7d) allows excluding both the incorporation of CuNpx-dmso crystal particles and the existence of physical mixture of CuNpx-dmso and CTb. The CTb/CuNpx XRD pattern was also compared to that of HNpx (Fig. 7e) to evaluate the possibility of incorporation of non-coordinated naproxen eventually originated from ligand dissociation process. Although the 2θ value (6.7°) of the first peak of HNpx is very close to that found for the new material, the highest intensity peaks of the organic crystalline drug were not found in the XRD pattern of CTb/CuNpx. Therefore, a reasonable explanation for the appearing of the peak at 6.9° might be an effect on the planes assigned to hydrated crystals due to the presence of the loaded copper-drug. The lower 2θ value suggests a higher interplanar distance that would agree with the presence of molecules with bigger size than water in the structure of the chitosan.

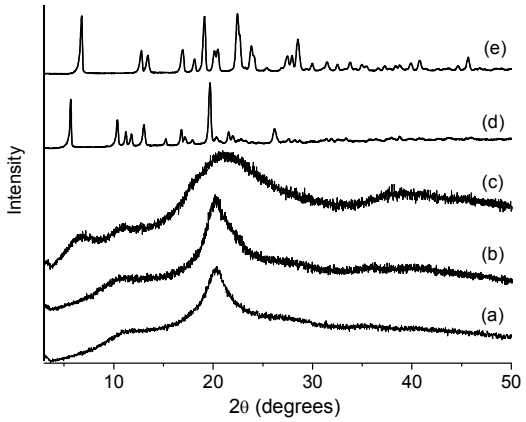

Fig. 7. XRD patterns of: (a) CT (dried commercial chitosan); (b) CTb non-loaded-beads; (c) CTb/CuNpx hybrid material; (d) CuNpx-dmso; (e) HNpx.

3.7. Thermal Analysis

The thermal analysis data for non-loaded CTb, CTb/CuNpx hybrid material and CuNpx-dmso are listed in Table 1. Fig. 8 shows the TG, DTG and DSC curves for CTb/CuNpx. The non-loaded CTb exhibits three main events of mass loss. The DTG peak at ~ 120 °C (12.2 % mass loss, endothermic) may be associated to the release of surface adsorbed water (m/z 18) while the second DTG peak at 287, 298 °C (50.5 % mass loss, exothermic) mostly associated to m/z 18 fragment, may result from groups involved in stronger interactions within the CT chains. The third DTG peak at 610 °C (35.5 % mass loss, highly exothermic) is mostly related to m/z 44 fragment that is typical of CO_2, and may be associated to the degradation of the CT chains. The CTb/CuNpx hybrid material shows distinct thermal behaviour. The first event at DTG peak 130 °C (7.3 % mass loss, endothermic) may be due to the release of surface adsorbed water. The second event at 205 °C (10.3 % mass loss) followed by a peak at 257 °C (31.0 % mass loss) (exothermic, both of them involving mostly release of m/z 18 fragment) might be predominantly associated to the degradation of naproxen (calc. value based on the composition of the hybrid material was ~ 35 %). In the case of the CuNpx-dmso complex, the first DTG peak at 150 °C (13.0 % mass loss) may be assigned to the dmso release, which is followed by the naproxen drug degradation, which occurs at 210-285 °C (55.4 % mass loss) and continues up ~ 600 °C (17.3 % mass loss at 300-600 °C), to give ~ 14 % final residual mass that corresponds to 2 mol of CuO (calc. 13.3 %). The further event at temperature above 300 °C for the CTb/CuNpx hybrid material (44.6 % mass loss, highly exothermic, releasing m/z 18 and 44 fragments) may be associated to the CT chain degradation. The CTb/CuNpx hybrid material (excluding the event at ~ 257 °C) showed ~ 61 % total mass loss, a value that is very close to the contribution of CT (65 %) found for its estimate experimental composition. The findings suggest that the degradation of CT is affected by the presence of the copper-drug. The main step of CT degradation for CTb/CuNpx occurs at the range 300-500 °C, while CTb shows two steps (265-500 °C; ~ 600 °C) associated to this process. The non-loaded CTb shows a high intensity signal for the m/z 18 fragment at ~ 300 °C, while the m/z 44 signal predominates at about 600 °C. In contrast, the main step of CT degradation for CTb/CuNpx at 300-500 °C involves release of both m/z 18 and m/z 44 fragments. Taking into account that m/z 18 fragment can also result from NH_3, it is plausible to consider that the total breakage of the biopolymer chains in CTb/CuNpx may involve release of both C- and N-fragments, at the same temperature range. Moreover, the non-loaded CTb releases N-fragment at lower temperature than it releases C-fragments. These differences might be associated to the involvement of the $–NH_2$ amino groups on interactions with the copper-drug within the CTb/CuNpx hybrid material. Additionally, the final mass (6.9 %) found for CTb/CuNpx may have high contribution of CuO residue originated from the loaded copper-drug (calc. 5.6 %).

Table 1. Thermal analysis data.

Compound or material	Temperature range (°C)	Main DTG peak (°C)	Mass loss (%)	Main fragments (m/z)*
Non-loaded CTb	30-265	~ 120	12.2	18
	265-500	287, 298	50.5	18 (>), 44
	500-700	610	35.5	18, 44 (>)
CTb/CuNpx	30-70	~ 130	7.3	18
	70-300	205	10.3	18 (>), 44
		257	31.0	18 (>), 44
	300-600	345, 378 410, 432	44.6	18, 44
CuNpx-dmso	30-200	150	13.0	48, 64, 78
	200 - 300	210, 255, 285	55.4	18 (>), 44
	300 - 600	364, 410, 486, 536	17.3	18, 44

* m/z 18: H_2O and/or NH_3; m/z 44: CO_2; m/z 48: SO; m/z 64: SO_2; m/z 78: dmso.

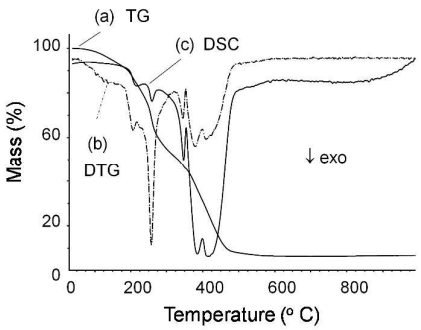

Fig. 8. (a) TG, (b) DTG and (c) DSC curves for the CTb/CuNpx hybrid material.

3.8. Behavior of the CTb/CuNpx hybrid material in gastric/intestinal pH simulated solutions

The CTb/CuNpx hybrid material was investigated for its behavior in gastric/intestinal pH simulated solutions to verify potential releasing properties. The monitoring made by HPLC revealed a peak with retention time between 5-6 min (see representative chromatograms in Fig. 9) typical of naproxen. The electronic spectrum of the species associated to this peak also confirmed the release of the organic drug from the hybrid material. The uncoated CTb/CuNpx loaded-beads showed a fast release rate for naproxen, associated to ~ 55 % release of the organic drug, in the first 2 h, at pH 1.2 (Fig. 10), which is probably related to the degradation of the chitosan in acidic solution. To avoid degradation of the biopolymer at low pH, the CTb/CuNpx hybrid material was coated with Acrycoat S100. This methacrylic acid copolymer is pH-dependent, resistant to gastric fluid (low pH) but freely soluble in the intestinal tract, and has been used in formulations, *e.g*., formulation of chitosan beads of drugs for colon targeting. [57] The acrycoat-coated CTb/CuNpx beads were investigated for the release behavior in gastric/intestinal simulated condition, *i.e*., sequentially, first at pH 1.2 to simulate average gastric emptying time for 2 h; then at pH 6.8 to mimic average intestinal transit time for 3 h; and finally at pH 7.4 corresponding to ileocecal pH for 3 h. [58] The coated hybrid material revealed capacity for releasing naproxen according to the cumulative drug release shown in Fig. 10. The acrycoat-coated beads exhibited significant decrease on the drug release rate (~ 20 % total released drug) in relation to the corresponding uncoated beads (~ 55 %) at simulated gastric pH, in 2 hours. The distinct drug release profile found for the hybrid material at low pH confirms the positive coating effects of Acrycoat. Additionally, peaks which could be assigned to chitosan species (see representative chromatogram in Fig. 9a) revealed that CT degradation was not highly significant for the coated-hybrid material at this pH. A burst release occurred at the first 10 min when the pH was raised from 1.2 to 6.8 (Fig. 10) probably due to the dissolution of the Acrycoat. The system continued to release naproxen slowly in the sequence of intestinal simulated condition in the subsequent hours. The % drug released (see representative chromatogram in Fig. 9b) at pH 6.8 in 3 hours was ~ 40 %. After changed pH to 7.4, in the following 3 hours, only additional 10 % naproxen was released (see representative chromatogram in Fig. 9c). The total % drug released in the sequential gastric/intestinal pH simulated solutions was ~ 70 %. This value was close to the total amount (75 %) of naproxen released in the next 16 hours (up to complete 24 h experiment) at pH 7.4 (see representative chromatogram in Fig. 9d), indicating that the hybrid material achieved the maximum organic drug release capacity at the end of the 8 h in sequentially increased pH conditions. The naproxen release behavior found for the coated CTb/CuNpx beads approaches the profile reported for a naproxen-eudragit nanoparticle formulation. [59] Therefore, the findings suggest that the coated CTb/CuNpx hybrid material is capable of releasing naproxen in a sustained release way for at least 24 h (following the initial burst release at pH 6.8) and, consequently shows capacity for delivering the organic drug over a prolonged period of time. The final solid material retained after the drug release process showed ~ 3 % Cu content (ICP-AES). This result indicates that the hybrid material also released metal, and that the release of copper and naproxen followed the molar ratio 1 Cu : 2 Npx. Interesting, the released Cu : naproxen molar ratio agrees with that of the $[Cu_2(Npx)_4]$ composition. Since the HPLC experiments indicated the presence of free naproxen drug in the gastric/intestinal pH simulated solutions, it might be assumed that copper and naproxen are released individually, rather than in the form of metal-drug complex at the investigated experimental conditions. Evidences from characterization discussed here pointed towards the entrapment of the CuNpx dinuclear complex into CTb. Therefore it could be suggested that the CTb-entrapped-CuNpx may undergo dissociation during the release experiments, or that the CTb/CuNpx hybrid material already contains different entrapped species. In addition to CTb-(NH_2)-$[Cu_2(Npx)_4]$ species, resulting from the CTb interaction with the dinuclear complex, other possible species, such as CTb-(NH_2)-$[Cu(Npx)_2]$, resulting from the CTb interaction with mononuclear species originated from dinuclear complex breakage, and/or CTb-(NH_2)-Cu + CTb-Npx, resulting from CTb individual interactions with copper and naproxen, cannot be ruled out. Attempts to investigate the stability of the original $[Cu_2(Npx)_4(dmso)_2]$ complex at similar conditions were made. Despite the poor solubility of the compound, it was possible to observe by electronic spectroscopy and HPLC that the compound undergoes dissociation reaction with loss of the naproxen-ligands at pH 1.2. At the highest pH values (6.8 and 7.4), however, most of the complex remained insoluble, thus keeping its integrity as solid and losing only small amount of the naproxen ligands. Therefore, it was possible to conclude that the behavior of the entrapped-CuNpx in the hybrid material is very distinct of the behavior of the CuNpx-dmso original complex at similar pH conditions.

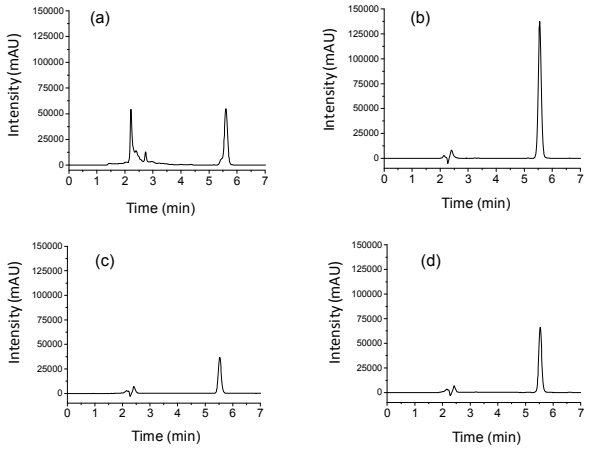

Fig. 9. Representative chromatograms of solutions from release experiment for coated CTb/CuNpx beads: (a) at pH 1.2 after 120 min, showing peaks assigned to CT (2-3 min) and to naproxen (5-6 min); (b) at pH 6.8 after 180 min, showing peak of naproxen; (c) at pH 7.4 after 180 min, showing peak of naproxen; (d) at pH 7.4 after 24 h, showing peak of naproxen.

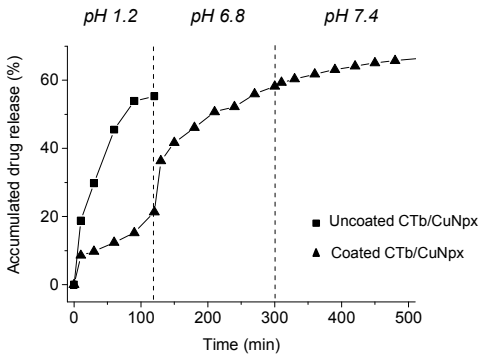

Fig. 10. Release profile for naproxen from uncoated CTb/CuNpx beads in simulated gastric pH, and from coated CTb/CuNpx beads in sequential simulated gastric/intestinal pH. Data for coated beads represent mean value of duplicate experiments.

4. Conclusions

Chitosan beads (CTb) are capable of interacting with the $[Cu_2(Npx)_4(dmso)_2]$ metallodrug. The loading capacity of CTb for CuNpx indicates a sponge-like behavior for copper-drug entrapping at CuNpx concentration range from 10^{-4} to 10^{-2} mol L^{-1}. A novel CTb/CuNpx hybrid material was prepared and characterized, and it was found to show distinct behavior from that of the corresponding non-loaded CTb. The interaction of CTb with the copper-drug may involve coordination of the metal ion to the amino groups the CT. The acrycoat-coated CTb/CuNpx beads show capacity for sustained releasing naproxen in sequential gastric/intestinal pH simulated conditions.

Conflict of interest

The authors declare they have no competing financial interest.

Acknowledgements

Authors gratefully acknowledge financial support from the Brazilian agencies: Fundação de Amparo à Pesquisa de São Paulo (FAPESP, research grants 2005/60596-8 and 2011/06592-1), Conselho Nacional de Desenvolvimento Científico e Tecnológico (CNPq, fellowships to Prof. D. de Oliveira Silva, and to D.J. Martins, I.M. Costa, A.C.P. Santos and R.G. Szszudlowski), and Coordenação de Aperfeiçoamento de Pessoal de Nível Superior (CAPES, fellowships to Hanif-Ur-Rehman and S.R.A. Rico). Authors also acknowledge C.R. Gordijo, R.Y.P. Alta, A.C.V. Négron, D. Petri, the group of Prof. H.E. Toma for experimental support, and Almapal S.A for donation of Acrycoat S100.

References

1 S. Kim, *Chitin, Chitosan, Oligosaccharides and Their Derivatives - Biological Activities and Applications*. NW: CRC Press Taylor & Francis Group, 2011.
2 G. A. F. Roberts, *Chitin Chemistry.* London: The Macmillan Press Ltda., 1992.
3 M. N. V. Ravi Kumar, R. A. A. Muzzarelli, C. Muzzarelli, H. Sashiwa and A. J. Domb, *Chem. Rev.,* 2004, 104, 6017-6084.
4 B. Sarmento and J. Neves, *Chitosan-Based Systems for Biopharmaceuticals - Delivery, Targeting and Polymer Therapeutics*. West Sussex: John Wiley & Sons, Ltd., 2012.
5 W. Xia, P. Liu, J. Zhang and J. Chen, *Food Hydrocolloids,* 2011, *25*, 170-179.
6 F. Brunel, N. E. E. Gueddari and B. M. Moerschbacher, *Carbohyd. Polym.,* 2013, 92, 1348-1356.
7 W. S. Wan Ngaha, L. C. Teonga and M. A. K. M. Hanafiaha, *Carbohyd. Polym.,* 2011, 83*,* 1446-1456.
8 S. Talebian, M. Mehrali, S. Mohan, H. R. B. Raghavendran, M. Mehrali, H. M. Khanlou, T. Kamarul, A. M. Afifi and A. A. Abas, *RSC Adv*., 2014, 4, 49144-49152.
9 P. S. Kumar, M. Selvakumar, S. G. Babu, S. K. Jaganathan, S. Karuthapandian and S. Chattopadhyay, *RSC Adv.*, 2015, 5, 57493-57501.
10 M. Garcia-Fuentes and M. J. Alonso, *J. Control. Release*, 2012, 161 496-504.
11 V. Bansal, P. K. Sharma, N. Sharma, O. P. Pal and R. Malviya*, Advan. Biol. Res.,* 2011, 5, 28-37.
12 N. Bhattarai, J. Gunn, M. Zhang, *Adv. Drug Delivery Rev*., 2010, 62, 83-99.
13 M. P. Patel, R. R. Patel and J. K. Patel. *J. Pharm. Pharmaceut. Sci.,* 2010, 13, 536-557.
14 J. H. Park, G. Saravanakumar, K. Kim and I. C. Kwon, *Adv. Drug Deliver Rev*., 2010, 62, 28-41.
15 S. A. Agnihotri, N. N. Mallikarjuna and T. M. Aminabhavi, *J. Control Release*, 2004, 100, 5-28.
16 L. Hu, Y. Suna, and Y. Wub, *Nanoscale*, 2013, 5, 3103-3111.
17 A. Bernkop-Schnürch and S. Dünnhaupt, *Eur. J. Pharm. Biopharm*., 2012, 81, 463-469.
18 R. Riva, H. Ragelle, A. Rieux, N. Duhem, C. Jérôme and V. Préat, *Adv. Polym. Science*, 2011, 244, 19-44.

19 S. G. Kumbar, A. R. Kulkarni and T. M Aminabhavi, *J. Microencapsul.,* 2002, 19, 173-180.
20 R. Shukla, J. Gupta, P. Shukla, P. Dwivedi, P. Tripathi, S. M. Bhattacharyab and P. R. Mishra, *RSC Adv*., 2015, 5, 69047-69056.
21 P. Mura, N. Zerrouk, A. Mennini, F. Maestrelli and C. Chemtob, *Eur. J. Pharm. Sci.,* 2003, 19, 67-75.
22 G. N. Kousalya, M. R. Gandhi, N. Viswanathan and S. Meenakshi, *Int. J. Biol. Macromol.,* 2010, 47, 583-589.
23 C. M. Futalana, C. Kanb, M. L. Dalidac, K. Hsienb, C. Pascuad and M. Wanb, *Carbohyd. Polym.*, 2011, 83, 528-536.
24 Z. Modrzejewska, *React. Funct. Polym.*, 2013, 73, 719-729.
25 A. D. Tiwari, A. K. Mishra, S. B. Mishra, A. T. Kuvarega and B. B. Mamba, *Carbohyd. Polym.*, 2013, *92*, 1402-1407.
26 X. Wang; D. Wang; P. Liang and X. Liang, *J. Appl. Polym. Sci.*, 2013, 128, 3280-3288.
27 H. Liu and C. Wang, *RSC Adv*., 2014, 4, 3864-3872.
28 T. Baran, A. Mentes and H. Arslan, *Int. J. Biol. Macromol*., 2015, 72, 94-103.
29 A. S. Kumari and D. D. Pathak, *Tetrahedron Lett.*, 2015, 56, 4135-4142.
30 A. Manikandan and Muthukrishnan Sathiyabama, *J. Nanomed. Nanotechnol.,* 2015, 6, 1-5
31 J. R. J. Sorenson, *Biology of copper complexes*. New York: Humana Press, 1987.
32 A. Andrade, S. F. Namora, R. G. Woisky, G. Wiezel, R. Najjar, J. A. A. Sertié and de Oliveira Silva, D. *J. Inorg. Biochem.* 2000, 81, 23-27
33 J. E. Weder, C. T. Dillon, T. W. Hambley, B. J. Kennedy, P. A. Lay, J. R. Biffin, H.L. Regtop and N.M. Davies, *Coord. Chem. Rev.,* 2002, 232, 95-126.
34 F. Dimiza, F. Perdih, V. Tangoulis, I. Turel, D. P. Kessissoglou and G. Psomas, *J. Inorg. Biochem.,* 2011, 105*,* 476–489.
35 D. de Oliveira Silva, *Anticancer Agents Med. Chem.*, 2010, 10, 312-323.
36 G. Ribeiro, M. Benadiba, A. Colquhoun and D. de Oliveira Silva, *Polyhedron*, 2008, 27, 1131-1137.
37 M. Benadiba, R. R. Santos, D. de Oliveira Silva and A. Colquhoun, *J. Inorg. Biochem.*, 2010, 104, 928-935.
38 M. R. Griffin and J. M. Sheiman, *Am. J. Med.*, 2001, 110, S33-S37.
39 http://www.ceva.com.au/Products/Products-list/CU-ALGESIC-R-Equine-Paste, accessed on august 16, 2015.
40 C. R. Gordijo, C. A. S. Barbosa, A. M. C. Ferreira, V. R. L. Constantino and D. de Oliveira Silva, *J. Pharm. Sci.,* 2005, 94, 1135-1148.
41 M. L. Lorenzo-Lamosa, C. Remuñán-López, J. L. Vila-Jato and M. J. Alonso, *J. Control Release*, 1998, 52, 109-118.
42 The United States Pharmacopoeia, 35th ed. Rockville: United States Pharmacopoeial Convention, 2012.
43 C. Dendrinou-Samara, D. P. Kessissoglou, G. E. Manoussakis, D. Mentzafos and A. Terzis, *J. Chem. Soc., Dalton Trans.*, 1990, 959-965.
44 C. Dendrinou-Samara*,* P. D. Jannakoudakis, D. P. Kessissoglou, G. E. Manoussakis, D. Mentzafos and A.Terzis, *J. Chem. Soc. Dalton Trans*., 1992, 3259-3264.
45 L. Zhang, P. Li, Y. Li and A. Wang, *Drug Dev. Ind. Pharm.,* 2012, 38, 872-882.
46 M. Kato and Y. Muto, *Coord. Chem. Rev*., 1988, 92, 45-83.
47 B. Kozlevcar, N. Lah, S. Makuc, P. Šegedin and F. Pohleven, *Acta Chim. Slov*., 2000, 47, 421-434.
48 P. Kögerler, P. A. M. Williams, B. S. Parajón-Costa, E. J. Baran, L. Lezama, T. Rojo and A. Müller, *Inorg. Chim. Acta*, 1998, 268*,* 239-248.
49 M. Kyuzou, W. Mori and J. Tanak, *Inorg. Chim. Acta*, 2010, 363*,* 930-934.
50 N. R. Kildeeva, P. A. Perminov, L. V. Vladimirov, V. V. Noviko and S. N. Mikhailov, *Russ. J. Bioorg. Chem.,* 2009, 35, 360-369.
51 S. Mekahlia and B. Bouzid, *Phys. Procedia*, 2009, 2, 1045-1053.
52 G. B. Deacon and R. J. Phillips, *Coord. Chem. Rev.,* 1980, 33, 227-250.
53 G. L. Clark and A. F. Smith, *J. Phys. Chem.*, 1937, 40, 863-879.
54 F. S. Kittur, A. B. V. Kumar and R. N. Tharanathan, *Carbohyd. Res*., 2003, 338, 1283-1290.
55 K. Ogawa, *Agric. Biol. Chem*., 1991, 55, 2375-2379.
56 K. Okuyama, K. Noguchi, T. Miyazawa, T. Yui and K. Ogawa, *Macromolecules*, 1997, 30*,* 5849-5855.
57 D. V. Kumar, A. Mishra and T. S. Easwari, *Europ. J. Appl. Sci.,* 2013, 5, 47-52.
58 N. C. Obitte, A. Chukwu and I. V. Onyishi, *Int. J. Appl. Res. Nat. Prod.*, 2010, 3, 1-17.
59 K. Adibkia, Y. Javadzadeh, S. Dastmalchi, G. Mohammadi, F. K. Niri and M. Alaei-Beirami, *Colloid Surface B,* 2011, 83, 155-159.